

PAPER • OPEN ACCESS

Cosmic ray acceleration in accretion flows of galaxy clusters

To cite this article: V.N. Zirakashvili and V.S. Ptuskin 2019 *J. Phys.: Conf. Ser.* **1181** 012033

View the [article online](#) for updates and enhancements.

You may also like

- [Thermoelastic non-stationary fields in a rigidly fixed plate](#)
Zh M Kusaeva
- [The dispute resolution of the authority of state institutions in Indonesia](#)
P R Capella, I S Putra, W S Widiarty et al.
- [Possible explanation of results of CR investigations in the energy interval \$10^{15}\$ – \$10^{17}\$ eV: Nuclear-physical approach](#)
A A Petrukhin and A G Bogdanov



ECS
The
Electrochemical
Society
Advancing solid state &
electrochemical science & technology

DISCOVER
how sustainability
intersects with
electrochemistry & solid
state science research

Cosmic ray acceleration in accretion flows of galaxy clusters

V.N.Zirakashvili, V.S.Ptuskin

Pushkov Institute of Terrestrial Magnetism, Ionosphere and Radiowave Propagation, 108840
Moscow Troitsk, Russia

E-mail: zirak@izmiran.ru

Abstract. We investigate acceleration of cosmic rays by shocks and accretion flows in galaxy clusters. Numerical results for spectra of accelerated particles and nonthermal emission are presented. It is shown that the acceleration of protons and nuclei in the nearby galaxy cluster Virgo can explain the observed spectra of ultra high energy cosmic rays.

1. Introduction

Clusters of galaxies are considered as a possible candidate for the origin of ultra-high energy cosmic rays (UHECRs) (see e.g. [1] for a review). Primordial density fluctuations are amplified via gravitational instability in the expanding Universe and result in the appearance of different coherent density structures at the present epoch. The galaxy clusters are formed at the latest times and continue to grow presently due to accretion of the circumcluster gas and dark matter. The inflow of matter is accompanied by an accretion shock at a distance of several Mpc from the cluster center.

Virgo cluster of galaxies with the total mass of $\sim 10^{15} M_{\odot}$ at the distance $d \sim 15 - 20$ Mpc [2] from the Milky Way is the nearest large galaxy cluster. It is located at the center of the Local super cluster of galaxies. Because of its proximity Virgo has been proposed as the source of observed UHECRs within a phenomenological diffusive model [3].

The diffusive shock acceleration (DSA) process [4, 5, 6, 7] is believed to be the principal mechanism for the production of galactic cosmic rays (CR) in supernova remnants (SNRs). Over the last decade the excellent results of X-ray and gamma-ray astronomy have been providing evidence of the presence of multi-TeV energetic particles in these objects (see e.g. [8]).

Since the accretion shocks are very large they can accelerate particles to significantly higher energies compared to SNRs and produce a significant fraction of observable UHECRs [9, 10, 11]. In this paper we describe the modifications of our non-linear DSA model [12] designed for the investigation of DSA in SNRs and apply it for the investigation of particle acceleration in clusters of galaxies. In particular we apply the model for the Virgo cluster of galaxies.

2. Nonlinear diffusive shock acceleration model

Details of our model of nonlinear DSA can be found in [12]. The model contains coupled spherically symmetric hydrodynamic equations and the transport equations for energetic protons, ions and electrons.



The hydrodynamical equations for the gas density $\rho(r, t)$, gas velocity $u(r, t)$, gas pressure $P_g(r, t)$, magnetic pressure $P_m(r, t)$, and the equation for isotropic part of the cosmic ray proton momentum distribution $N(r, t, p)$, the momentum per nucleon distribution $N_i(A, r, t, p)$ of nuclei with atomic number A and dark matter velocity distribution $F(r, t, w)$ in the spherically symmetrical case are given by

$$\frac{\partial \rho}{\partial t} = -\frac{1}{r^2} \frac{\partial}{\partial r} r^2 u \rho \quad (1)$$

$$\frac{\partial u}{\partial t} = g(r) - u \frac{\partial u}{\partial r} - \frac{1}{\rho} \left(\frac{\partial P_g}{\partial r} + \frac{\partial P_c}{\partial r} + \frac{\partial P_m}{\partial r} \right) \quad (2)$$

$$\frac{\partial P_g}{\partial t} + u \frac{\partial P_g}{\partial r} + \frac{\gamma_g P_g}{r^2} \frac{\partial r^2 u}{\partial r} = -(\gamma_g - 1) \Lambda_c(T_e) n^2 \quad (3)$$

$$\frac{\partial P_m}{\partial t} + u \frac{\partial P_m}{\partial r} + \frac{\gamma_m P_m}{r^2} \frac{\partial r^2 u}{\partial r} = 0 \quad (4)$$

$$\begin{aligned} \frac{\partial N}{\partial t} = \frac{1}{r^2} \frac{\partial}{\partial r} r^2 D(p, r, t) \frac{\partial N}{\partial r} - u \frac{\partial N}{\partial r} + \frac{\partial N}{\partial p} \frac{p}{3r^2} \frac{\partial r^2 u}{\partial r} + \frac{1}{p^2} \frac{\partial}{\partial p} p^2 b(p) N + 4\nu_{ph}(4) N_i(4) \\ + \sum_{A=5}^{56} \nu_{ph}(A) N_i(A) \end{aligned} \quad (5)$$

$$\begin{aligned} \frac{\partial N_i(A)}{\partial t} = \frac{1}{r^2} \frac{\partial}{\partial r} r^2 D_i(p, r, t) \frac{\partial N_i(A)}{\partial r} - u \frac{\partial N_i(A)}{\partial r} + \frac{\partial N_i(A)}{\partial p} \frac{p}{3r^2} \frac{\partial r^2 u}{\partial r} + \frac{1}{p^2} \frac{\partial}{\partial p} p^2 b(p) N_i(A) \\ - \nu_{ph}(A) N_i(A) + \nu_{ph}(A+1) N_i(A+1) \end{aligned} \quad (6)$$

$$\frac{\partial F}{\partial t} = -\frac{1}{r^2} \frac{\partial}{\partial r} r^2 w F - g(r) \frac{\partial F}{\partial w} \quad (7)$$

Here $P_c = 4\pi \int dp p^3 v(N + \sum_A A N_i(A))/3$ is the cosmic ray pressure, T_e , γ_g and n are the gas temperature, adiabatic index and number density respectively, γ_m is the magnetic adiabatic index, $D(r, t, p)$ is the cosmic ray diffusion coefficient. The radiative cooling of gas is described by the cooling function $\Lambda_c(T_e)$.

The gravitational acceleration $g(r)$ is given by the following expression

$$g(r) = \Lambda r - \frac{4\pi G}{r^2} \int_0^r r_1^2 dr_1 (\rho(r_1) + \rho_{DM}(r_1)) \quad (8)$$

where G is the gravitational constant, Λ is the lambda term and $\rho_{DM}(r) = \int dw F(r, w)$ is the dark matter density.

The function $b(p)$ describes the energy losses of particles. In particular the losses of multi EeV protons and nuclei via electron-positron pair production on the microwave background radiation (MWBR) are important in galaxy clusters. Another losses of energy of the nuclei occur in photonuclear reactions with infrared photons. They are described by two last terms in Eq. (6). We use a simplified approach and assume that the nuclei lose one nucleon in every

photonuclear reaction with the rate $\nu_{ph}(A)$. The corresponding proton source term is added in Eq. (5). For the calculation of photonuclear cross-sections we use the background spectrum of infrared photons $n(\epsilon) = 0.87 \cdot 10^{-3} a^{-4}(t) \epsilon^{-2} \text{ cm}^{-3} \text{ eV}^{-1}$, where ϵ is the photon energy expressed in eV and $a(t)$ is the expansion factor of the Universe. At the present epoch ($a = 1$) the spectrum is three times lower than LIR spectrum of Puget et al. [13] and is close to the lower limit of Malkan & Stecker [14].

Cosmic ray diffusion is determined by particle scattering on magnetic inhomogeneities. Here we consider the simplest model with strong background random magnetic fields in the circumcluster medium. The properties of the gas and magnetic field in the circumcluster medium are determined by galactic winds of individual galaxies. These winds were strong in past when the star formation rate was significantly higher than at the present epoch. The winds were driven by cosmic rays and hot gas produced by supernova explosions. The gas was heated, galactic cosmic rays were reaccelerated and magnetic fields were amplified at termination shocks of the galactic winds. That is why we expect that these three components have comparable energy densities in the circumcluster medium. Additionally the galactic winds transport metals and therefore the metallicity of the circumcluster medium is different from the primordial one that is indeed observed.

Bearing in mind that the magnetic field is strong in the circumcluster medium we neglect its generation via cosmic ray streaming instability in Eq. (4). We also neglect the gas heating via magnetic dissipation in Eq. (3). So the gas and magnetic pressures P_g and P_m evolve in accordance with adiabatic compression of the gas. Below we use the magnetic adiabatic index $\gamma_m = 3/2$.

We use Bohm-like dependence of the diffusion coefficient D of energetic particles with the charge q , momentum p and speed v

$$D = \eta_B D_B, \quad D_B = \frac{cpv}{3qB}, \quad B = \sqrt{8\pi P_m} \quad (9)$$

where B is the total magnetic field strength, while η_B is a free parameter characterizing speed of diffusion in the terms of Bohm diffusion. Since the Bohm diffusion coefficient D_B is the minimal possible value we shall use the value of $\eta_B = 2$ below.

In the shock transition region the magnetic pressure is increased by a factor of σ^{γ_m} , where σ is the shock compression ratio. Its impact on the shock dynamics is taken into account via the Hugoniot conditions.

We do not consider the injection of thermal ions at the shock front in the present study. As was mentioned before there are background cosmic rays in the circumcluster medium. We assumed that the spectrum of these particles is given by

$$N_{IG}(p) = N_0 \left(\frac{a(t)p}{p_{IG}} \right)^{-\gamma-2} \exp \left(-\frac{a(t)p}{p_{IG}} \right) \quad (10)$$

Here p_{IG} is the maximum momentum of background cosmic rays at the present epoch and γ is the spectral index of differential energy distribution of background cosmic rays.

The similar expression was used for the background spectra of nuclei. Helium nuclei were taken 10 times less abundant than protons. For heavier nuclei we assumed an enrichment proportional to the atomic number A as observed in Galactic cosmic rays.

The following expressions were used for the circumcluster magnetic and gas pressures

$$P_{gIG} = a(t)^{-3\gamma_g} P_{g0}, \quad P_{mIG} = a(t)^{-3\gamma_m} P_{m0}, \quad (11)$$

where P_{g0} and P_{m0} are the gas and magnetic circumcluster pressures at the present epoch respectively.

3. Modeling of DSA in the Virgo cluster

We model the Virgo cluster formation and particle acceleration for the cosmological parameters $\Omega_b = 0.05$, $\Omega_{DM} = 0.25$, $\Omega_\Lambda = 0.7$ and the Hubble constant $H = 70 \text{ km s}^{-1} \text{ Mpc}^{-1}$. The corresponding mean barion density ρ_b of the Universe is $\rho_b = 3\Omega_b H^2 / 8\pi G = 4.6 \cdot 10^{-31} \text{ g cm}^{-3}$. The lambda term in Eq. (8) is given by $\Lambda = \Omega_\Lambda H^2$. The initial instant of time is $t_0 = 4 \text{ Gyr}$ from the Big Bang.

The parameters of the background cosmic ray spectrum given by Eq. (10) were adjusted to reproduce observations of Auger Collaboration. We used the values $\gamma = 1.8$ and $p_{IG} = 8 \text{ PeV}/c$. The spectra of background cosmic rays are somewhat harder than the expected spectra of galactic sources. However the additional reacceleration at galactic wind termination shocks indeed will make galactic cosmic ray spectra harder.

We use the initial condition corresponding to the self-similar solution of Bertschinger [15]. At latest times the accelerated expansion of the Universe results in the higher accretion shock speed and radius in comparison with this solution.

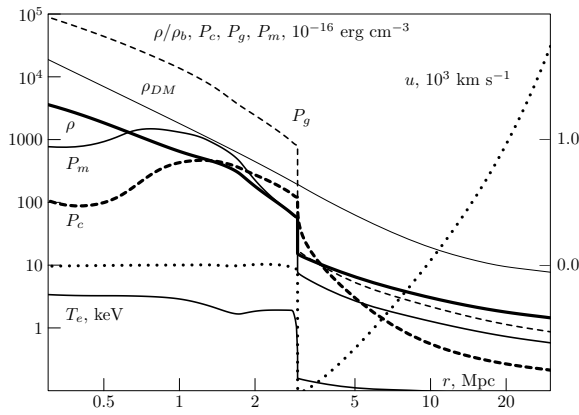


Figure 1. The radial dependence of the gas density (thick solid line), dark matter density (thin dotted line), the gas velocity (dotted line), cosmic ray pressure $B^2/8\pi = P_m$ (solid line), the gas temperature T_e (thin solid line) and the gas pressure P_g (dashed line) at $t = 13.5 \text{ Gyr}$ in the Virgo cluster.

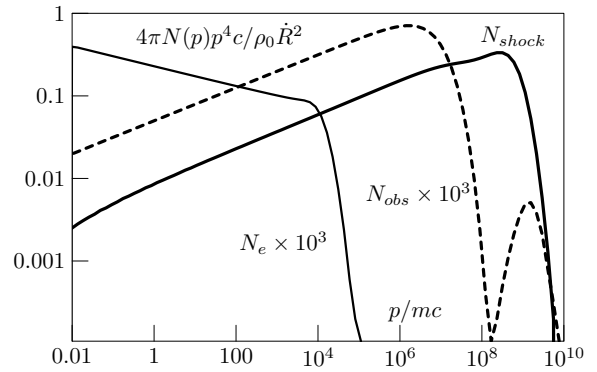


Figure 2. Spectra of accelerated particles at the accretion shock of Virgo cluster. The spectrum of protons (thick solid line) and electrons (thin solid line) are shown. We also show the proton spectrum at the Milky Way position at $r = 20 \text{ Mpc}$ (dashed line).

Figures (1)-(5) illustrate the results of our numerical calculations.

The radial dependence of physical quantities in the Virgo cluster at the present epoch ($t = 13.5 \text{ Gyr}$) are shown in Fig.1. At large distances we have the uniform expansion of the Universe. Closer to the cluster deviations from the Hubble law due to the initial local overdensity occur. We observe an inflow of matter inside a so-called "turnaround" point at $r \approx 10 \text{ Mpc}$. The accretion shock is situated at $r = R = 3 \text{ Mpc}$. The gas temperature is several keV inside the shock. The calculated gas density profile is in agreement with observations of the Virgo cluster [2]. The total mass of the gas inside the shock $1.5 \cdot 10^{14} M_\odot$ is also close to the observed value [2].

The cosmic ray, magnetic and gas pressures at large distances are of the order of $10^{-16} \text{ erg cm}^{-3}$ that is considered as a characteristic value for the extragalactic pressure around the Milky Way. The corresponding strength of the background magnetic field is $B_{IG} = 3 \cdot 10^{-8} \text{ G}$ that is a reasonable value for the Local supercluster.

It is interesting that the adjusted level of background cosmic rays results in the pressure of reaccelerated particles close to 10% of the ram pressure of the accretion shock. This number is

similar to the one found in the hybrid modeling of collisionless quasiparallel shocks [16] where the ions are injected at the shock front.

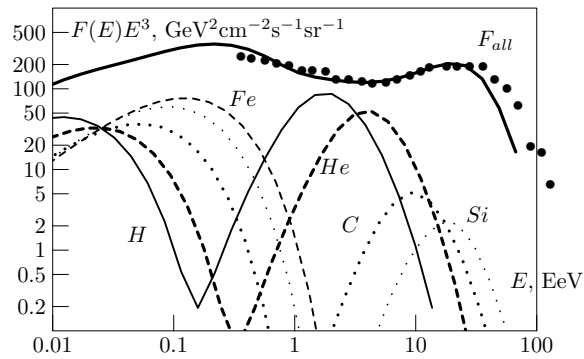


Figure 3. Calculated all-particle spectrum (thick solid curve), the spectrum of protons (thin solid line) and the spectra of other nuclei at the Milky Way position. Observational data of Auger Collaboration [17] (circles) are also shown.

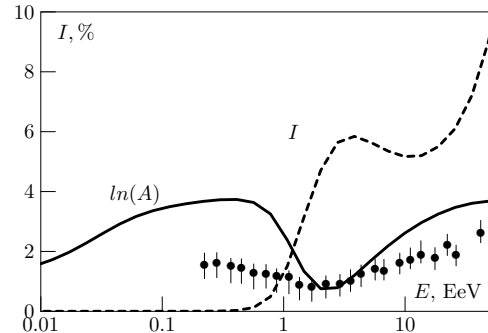


Figure 4. Calculated mean logarithm (solid line) and cosmic ray anisotropy (dashed line) at the Milky Way position. Experimentally measured mean logarithm data of Auger collaboration [17] using EPOS-LHC model of particle interactions in the atmosphere (data with error-bars) are also shown.

Spectra of accelerated in Virgo protons and electrons at $t = 13.5$ Gyr are shown in Fig.2. At this point the maximum energy of accelerated protons is close to 10^{18} eV. Only highest energy protons and nuclei from the cut-off region reach the Milky Way. Lower energy particles simply have not time to propagate from the shock surface to the Milky Way. We can observe only exponentially small fraction of protons (10^{-4}) reaccelerated at the accretion shock. So the particles are in a rather unusual propagation mode (see also [10]). At lower energies we observe the background circumcluster cosmic rays.

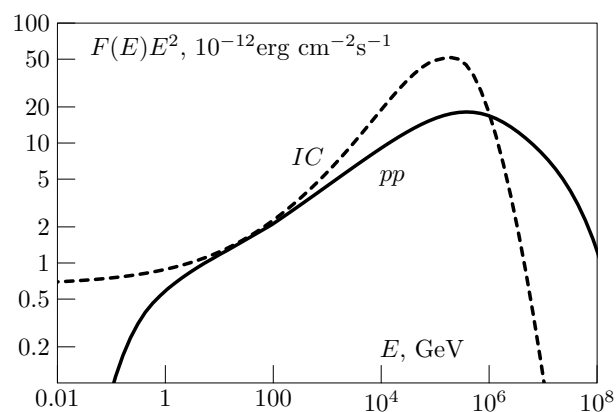


Figure 5. The results of modeling of gamma radiation of Virgo. We show IC emission (dashed line) and gamma-ray emission from pion decay (solid line). The absorption of multi-TeV photons due to pair production is not taken into account.

All-particle spectrum and spectra of individual nuclei calculated for the Milky Way position ($r = 20$ Mpc) are shown in Fig.3. The ankle at 5 EeV corresponds to the transition from the proton-Helium composition to the heavier nuclei dominated composition in our model. The heaviest nuclei do not present in the spectrum because of the photonuclear disintegration. The cut-off energy of the spectrum is mainly determined by the photonuclear reactions of heavy nuclei during acceleration and propagation. If we neglect the photonuclear reactions the maximum energy will be several times higher.

Calculated mean logarithm of atomic number and anisotropy are shown in Fig.4. The model reproduces light composition at EeV energies and the dipole anisotropy below the value of 6.5 percent measured by Auger Collaboration [18].

The spectra of unabsorbed gamma rays expected from the Virgo cluster are shown in Fig. 5. The gamma emission shows two components. One is produced by the nuclear collisions of protons and nuclei with gas in the cluster interior while another one is the inverse Compton component that at TeV energies is produced by electron positron pairs generated via interaction of accelerated particles with background photons of MWBR. The last process is rather efficient in galaxy clusters [19, 20]. In spite of the high expected flux the large angular size of the source (several degrees) makes the gamma detection of the Virgo cluster very difficult.

4. Discussion

We show that almost all UHECRs can be accelerated in the nearby Virgo cluster of galaxies. Our consideration is close to the earlier pure proton model of Kang et al. [10]. Note that we used more realistic value of the magnetic field strength that is 10 times lower. The corresponding decrease of the maximum energy is compensated by the presence of heavier nuclei in UHECR spectrum.

The drawback of the model is its sensitivity to adjusted parameters to fit UHECR data. As mentioned before we observe an exponentially small part (10^{-4}) of the highest energy particles accelerated at the accretion shock. That is why modest variations of the magnetic field strength result in the significant change of UHECR intensity.

Probably more massive and more distant clusters like Coma or another astrophysical sources (e.g. active galactic nuclei) also might give some contribution at highest energies. The particles accelerated in distant astrophysical objects can reach the Local supercluster propagating in the cosmological voids where the magnetic fields are very weak.

The adjusted maximum energy of background cosmic rays $E_{IG} = cp_{IG} = 8 Z$ Pev is not far from the "knee" energy. It is not excluded that this is not a coincidence. The value of E_{IG} is rather well constrained by available UHECR data. For lower values of E_{IG} we would observe a large dip in the spectrum between 0.1 and 1 EeV. For higher values of E_{IG} we would observe heavy UHECR composition at 1 EeV.

The work was supported by Russian Foundation of Fundamental Research grant 16-02-00255.

- [1] Brunetti G and Jones T 2014 *Intern. Journal of Modern Physics D* **29** 3007
- [2] Ade P A R, Aghanim N, Arnaud M. et al 2016, *Astron. Astrophys.* **596** 101
- [3] Giler M, Wdowczyk W and Wolfendale A W 1980 *J. Phys. G* **6** 1561
- [4] Krymsky G F 1977 *Soviet Physics-Doklady* **22** 327
- [5] Bell A R 1978 *MNRAS* **182** 147
- [6] Axford W I, Leer E and Skadron G 1977 *Proc. 15th ICRC, Ploudiv* **90** 937
- [7] Blandford R D and Ostriker J P 1978 *Astrophys. J.* **221** L29
- [8] Lemoine-Goumard M 2004 *Proc. IAU Symp.* **296** 287
- [9] Norman C A, Melrose D B and Achterberg A, 1995 *Astrophys. J.* **454** 60
- [10] Kang H, Ryu D and Jones T W 1996 *Astrophys. J.* **456** 422
- [11] Kang H, Rachen J P and Biermann P L, 1997 *MNRAS* **286** 257
- [12] Zirakashvili V N and Ptuskin V S 2012 *Astropart. Phys.* **39** 12
- [13] Puget J L, Stecker F W and Bredekamp J H 1975 *Astrophys. J.* **205** 638
- [14] Malkan M A and Stecker F W 1998 *Astrophys. J.* **496** 13
- [15] Bertschinger M 1985 *Astrophys. J. Suppl.* **58** 39
- [16] Caprioli D 2014 *Nuclear Physics B (Proc. Suppl.)* **256** 48
- [17] Letessier-Selvon A for the Pierre Auger Collaboration 2014 *Brazilian J. of Phys.* **44** 560 arXiv:1310.4620
- [18] Pierre Auger Collaboration 2017 arXiv:1709.0732
- [19] Vannoni G, Aharonian F A, Gabici S, Kelner S R and Prosekin A 2011 *Astron. Astrophys.* **536** 56
- [20] Inoue S, Sigle G, Miniati F and Armengaud E 2008 *Proc. 30th ICRC* **4** 555